Preprint
UCRL-JC-148502

E x B-Drift, Current, and Kinetic Effects on Divertor Plasma Profiles During ELMs

T.D. Rognlien, M. Shimada

This article was submitted to
15th International Conference on Plasma Surface Interactions in Controlled Fusion Devices, Gifu, Japan, May 27-31, 2002

May 23, 2002

U.S. Department of Energy
Lawrence
Livermore
National
Laboratory

E×B-Drift, Current, and Kinetic Effects on Divertor Plasma Profiles durings ELMs

T.D. Rognlien[1] and M. Shimada[2]

[1] *Lawrence Livermore National Laboratory, Livermore, California 94551 USA*
[2] *ITER International Team, ITER Naka Co-Center, Naka, Ibaraki-ken 311-0193, Japan*

Abstract

The transient heat load on divertor surfaces from Edge-Localized Modes (ELMs) in tokamaks can be very large and thus of concern for a large device such as ITER. Models for kinetic modfications to fluid models are discussed that should allow them to reasonably describe the long mean-free path regime encountered owing to the high electron and ion temperatures in the SOL during large ELMs. A set of two-dimensional (2D) simulations of the dynamic response of the scrape-off layer (SOL) plasma to an ELM is presented. The role of plasma currents and $\mathbf{E}\times\mathbf{B}$ motion is emphasized, which cause large changes in the response compared to models neglecting them.

1 Introduction

Edge Localized Mode (ELM) heat load on material surfaces is a key issue for burning-plasma tokamak experiments, *e.g.*, ITER and FIRE. According to the observations in existing tokamaks, the ELM heat flux on the divertor can have a profile width about twice that of the steady-state heat flux [1]. When the ELM occurs, the plasma with parameters close to those at the top of the so-called pedestal just inside the magnetic separatrix is assumed injected or connected to the open field-line SOL. Here, at least two processes occur. One change is the reduction in the plasma pressure gradients, which modifies the bootstrap current, and thus the poloidal magnetic flux surfaces, resulting in a shift of the magnetic separatrix defining the SOL. A second change is flow of the injected plasma to the divertor plates. In this paper, we focus on evaluating the latter process by including the effects of the $\mathbf{E}\times\mathbf{B}$ drifts and parallel flow dynamics, thus extending previous work [2,3] that neglects such effects.

The role of classical $\mathbf{E}\times\mathbf{B}$, diamagnetic drifts, and parallel currents in the SOL has been the subject of a number of theoretical and modeling studies, *e.g.*, [4,5], and corresponding experimental measurements [6]. For the high temperatures encountered during and just after an ELM, these effects should be stronger as they increase with temperature. While the ultimate goal is to understand the impact of large ELMs in big devices, in this short paper we focus on developing a clear physics picture of present transport models for more modest ELMs with parameters typical of present-day tokamaks; the DIII-D tokamak is used as a standard example. Indeed, we find that there is already a rich interaction of processes for this case.

The plan of the paper is as follows: The geometry and model are given in Sec. 2. Kinetic corrections to the fluid equations are given in Sec. 3, and time-dependent results for divertor profiles during an ELM are presented in Sec. 4 followed by a conclusions section.

2 Geometry, equations, and ELM model

We use the UEDGE 2D transport code [5] to calculate the plasma and neutral response to an ELM-like event. In order to focus on the essential physics, we consider a DIII-D single-null MHD equilibrium with the divertor plates being approximated by surfaces orthogonal to the magnetic flux surfaces. Equations are solved for ion particle continuity and parallel momentum, with the parallel direction being that along the magnetic field, $\mathbf{B}$. The current continuity equation is included for the electrostatic potential, ϕ, with ∇B and curvature drifts included and quasineutrality assumed. Separate electron and ion temperature equations are used. The hydrogen neutrals from a plate recycling coefficient of $R = 0.99$ are described by a diffusive model, *i.e.*, inertia and viscosity are neglected compared to the strong charge-exchange momentum transfer with ions.

The parallel transport is assumed to be classical [7] with flux-limits on the viscosity, thermal force, heat conductivity terms as discussed in more detail in Sec. 3. The pre-ELM cross-field transport is assumed to be enhanced owing to plasmas turbulence; we use a diffusive model here, although convection can also be used. In the pre-ELM state, radial diffusion coefficients used are in the range deduced from present experimental results [1]; for density of $D = 0.25$ m^2/s, for electron and ion energy transport, $\chi_{e,i} = 0.5$ m^2/s; radial ion viscosity for parallel and perpendicular velocities are also set to 0.5 m^2/s. The core-edge ion density is set to 3×10^{19} m^{-3} and the power into the SOL is 4 MW. At the divertor plates, the poloidal ion velocity, v_{ip}, into the plate is set by the condition $v_{ip} = (\mathbf{E} \times \mathbf{B}/B^2)_p + c_s B_p/B$ [8], where B_p/B is the ratio of the poloidal to total B-field, and c_s is the ion-acoustic speed.

The poloidal ion energy flux at the plate is $(5/2)v_{ip}nT_i$, where n is the plasma density and T_i the ion temperature. The poloidal electron energy flux is $n\bar{v}_e(2+e\phi_s/T_e)(B/B_p)\exp(e\phi_s/T_e)$, where $\bar{v}_e = (8T_e/\pi m_e)^{1/2}$, ϕ_s is the electostatic sheath potential, $-e$ the electron charge, and m_e the electron mass.

The ELM event is modeled by abruptly increasing the diffusion coefficients by a factor of 20 for a time to 200 μs in a broad region around the outer midplane, while the core-edge density is held fixed as are the core-edge temperatures at their pre-ELM values of $\sim$ 400 eV. The profile of the enhanced diffusion is a Gaussian shape in the poloidal direction, centered at the outer midplane and having a half-width of 1.9 m. In the radial direction, the enhanced diffusion is uniform to the separatrix and decays exponentially in the SOL with a scale-length of 1 cm.

3 Kinetic extensions for fluid models

The classical parallel transport coefficients given, for example, by Braginskii [7] need to be modified to account for the long mean-free path effects during ejection of hot plasma into the SOL. The most common procedure is to use flux limits. Here, the classical diffusive flux is limited to a fraction of the free-steaming flux. For example, the electron thermal flux is limited as follows:

$$q_c = -\kappa_e \frac{\partial T_e}{\partial s_\parallel} \rightarrow -\kappa_e \frac{\partial T_e}{\partial s_\parallel}[1 + (q_c/q_f)^2]^{-1/2}, \tag{1}$$

where T_e is the electron temperature, κ_e is the classical conductivity, $s_\parallel$ is the distance along $\mathbf{B}$, $q_f = c_e n T_e (2T_e/m_e)^{1/2}$, n is the plasma density, and m_e the electron mass. The coefficient $c_e \approx 0.15$ is obtained by comparisons with Monte Carlo calculations [9]. Similarly, for the ion conduction, $c_i \approx 0.15$, and a corresponding limit for the ion parallel viscosity uses a coefficient of $c_v = 0.5$.

A second correction that must be made is for the thermal force term appearing in the electron parallel momentum equation of the form $0.71n\nabla_\parallel T_e$. We adjust this term by multipling the term by $1/(1+\lambda/L_s)$, where L_s is the minimum of the connection length from the midplane to the plate, $L_\parallel$, or the parallel gradient length of T_e, and λ is the mean-free path for Coulomb collisions. The results to be presented are largely insensitive to this correction, even if the reduction is made more aggressive.

While details of flux limiting models can be inaccurate [10], we argue that during an ELM event, as the T_e values rise, the temperature profile becomes comparatively flat along $s_\parallel$, such that errors in the profile are relatively unimportant. This is the well-known sheath-limited regime, where the electron

energy loss at the divertor is given by

$$2T_e\Gamma_e = 2T_e n(\bar{v}_e/4)\exp(e\phi_s/T_e). \tag{2}$$

Here Γ_e is the electron particle flux. This point is illustrated in Fig. 1 where we show the time evolution of the poloidal (and thus $s_\parallel$) profile of T_e on a flux surface at 2 mm into the SOL measured at the midplane for the ELM model discussed in Sec. 4. Owing the exponential dependence, the most important factor setting Γ_e is the sheath potential.

Before considering a general model for the sheath potential, we need to extend the model of the sheath-limited regime to very long mean-free paths where the electron distribution function can become depleted in velocity space corresponding to the velocity region where single-transit escape is possible. Then velocity scattering into this region determines the electron loss rate. The loss rate for the transition from the sheath-limited regime to this velocity-space regime has been considered for mirror devices some years ago [12], and shows that the general electron particle flux escaping at the plate can be well approximated as

$$\Gamma_e \to \frac{n\bar{v}_e \exp(e\phi_s/T_e)}{4(1+\tau_p/\tau_c)}. \tag{3}$$

Here τ_p is long mean-free path confinement time [11], and τ_c is the confinement time for the collisional sheath-limited case [12]. In Eq. (3), the factor $\zeta \equiv 1/(1+\tau_p/\tau_c) \approx 1/[1+(\ln 2/2)(\lambda/L_\parallel)(e\phi_s/T_e)]$ gives smooth transition to the regime where electron loss is set by velocity-space diffusion from Coulomb collisions when $\tau_p > \tau_c$ [12]. The ions are not confined, so they flow out owing to their thermal velocity and the "ambipolar" electric field; however, reversal of the outward flow can arise from $\mathbf{E}\times\mathbf{B}$ and local source effects.

The sheath potential can now be calculated that includes both short and long mean-free path regimes. The parallel current through the sheath, J, must be the sum of the ion and electron contributions;

$$J = nec_s + nev_{\perp e}B/B_p - ne\zeta(\bar{v}_e/4)\exp(e\phi_s/T_e), \tag{4}$$

where the typically small second term arises from detailed consideration of the $\mathbf{E}\times\mathbf{B}$ and diamagnetic electron velocity $v_{\perp e}$ at the plate [8]. Inverting this equation gives the sheath potential as

$$-\frac{e\phi_s}{T_e} = \ln\left(\frac{\zeta\bar{v}_e/4\hat{c}_s}{1-J/J_{sat}}\right), \tag{5}$$

where $\hat{c}_s \equiv c_s + v_{perpe}B/B_p$, and $J_{sat} = ne\hat{c}_s$ is the ion saturation current. Note that ζ also depends on ϕ_s, but unless the edge temperature is very high, $\zeta \approx 1$. For $\zeta = 1$ and $J = 0$, Eq. (5) gives the familiar results of $e\phi_s/T_e \sim 3$ for deuterium. For the ELM simulations in the next section, we find regions where $J \sim J_{sat}$, which strongly affects ϕ_s.

4 Transport simulations during a simulated ELM

As mention in Sec. 2, the ELM is simulated by increasing the diffusion coefficients by a factor of 20 over a broad area encompassing the outer midplane for 200 μs. The response of T_e in the SOL can be seen in Fig. 1. Owing to the high-density, low T_e conditions at the inner plate, much of the T_e rise occurs at the outer plate in the first 50 μs; the inner leg temperature rises more slowly because electron convection (a current) carries most of the energy to the outer plate and because of the larger number of cold electrons in the inner divertor leg.

The effect of including the cross-field drifts ($\mathbf{E}\times\mathbf{B}$ and diamagnetic) and current is illustrated for the plasma density at the outer plate in Fig. 2. The three major peaks shown late in the ELM injection for no current or drifts is a complicated interplay of the time response to strong heat pulse from the ELM and the recycling neutrals leading to regions of local poloidal flow reversal. We have verified that the structure is not a numerical artifact by performing mesh resolution studies. Rather than focusing on this density structure, one should note from Fig. 2 that with drifts and current, the peaks largely disappear. Here the density decreases substantially from the pre-ELM state. The reason for this is large $\mathbf{E}\times\mathbf{B}$ poloidal flow reversal as will illustrated later in this section. Also note that the pre-ELM density is shifted to the left for the lower figure with $\mathbf{E}\times\mathbf{B}$; this can be explained by the radial $\mathbf{E}\times\mathbf{B}$ drift near the plate. For our case, direction of $\mathbf{B}$ is dominantly out of the plane of Fig. 2 (ion ∇B is downward), such that the normal downward poloidal electric field produces at drift of ions and electrons to the left, toward the private flux region.

A primary quantity of interest is the poloidal heat flux on the plate, as shown in Fig. 3 at $t = 200$ μs for the cases without and with drifts and currents. Here the heat flux is plotted versus poloidal flux, with unity corresponding to the separatrix. The strong density structure for the no drift case is only partially apparent because T_e has an opposite and partially compensating structure. The case with drifts shows very little fine structure, again in part from the T_e variation, but also from the substantial electron current which convects energy to the outer plate. Also note that the heat flux to the inner plate is significantly reduced when current is allowed. There is slight, but hardly

noteworthy, narrowing of the heat flux over the major heat-flux region when drifts are included.

The role of the $\mathbf{E}\times\mathbf{B}$ drifts during the ELM pulse can be understood from the vector plot of the ion flux×area shown in Fig. 4 at two times: (a), $t = 0$ s and (b), $t = 27$ μs. Initially, most of the ion current is directed toward the plate, although there is a large flow in the private flux region from the outer divertor to the inner divertor, as noted elsewhere. After the ELM pulse, the rapid rise in T_e and ϕ gives a stronger $\mathbf{E}\times\mathbf{B}$ poloidal flow causing flow reversal (ion flow up along both sides of the separatrix; this flow depletes the density near the plate, yielding the large drop seen in Fig. 2.

Finally, the effect of the parallel current is illustrated by considering the parameter $e\phi_s/T_e$ as given in Eq. (5) at each plate for two different times during the ELM simulation in Fig. 5. The current flows from the outer plate (higher plasma. Even though there is an electrical current initially ($t = 0$ s), it being directed away from the outer plate outside the separatrix (excess electrons flowing into the plate), the value of $e\phi_s/T_e$ is close to its zero current value of 2.8 at each plate. However, during the ELM pulse ($t = 200$ μs), these values change dramatically, as shown in the lower frame in Fig. 5. During the ELM, the magnitude and the width of the current increase. At the inner plate, electrons need to be suppressed from escaping, and at the outer plate, the low $e\phi_s/T_e$ is needed to allows sufficient electrons to carry the current through the sheath, both because the current is larger and the plasma density at the plate is lower. The different values of $e\phi_s/T_e$ have important consequence for the ion energy spectrum reaching the plate surface, since each ion acquires the sheath potential in transiting to the plates.

5 Conclusions

The influence of ELM ejection of plasma density and energy into the SOL is studied, with emphasis on the role of $\mathbf{E}\times\mathbf{B}$ drifts and plasma current. We present models of kinetic corrections to fluid equations to capture the main features of long mean-free path parallel transport during the high-temperature ELM-pulse. The effect of $\mathbf{E}\times\mathbf{B}$ drifts are most evident in the plasma near the divertor plate where a radial shifting and poloidal flow reversal occur owing to the high potential current the ELM. Much of the power to the outer divertor is carried by the electron current, which increases in magnitude and width during the ELM, causing a decrease in the normalize sheath potential ϕ_s/T_e at the outer divertor and in strong increase at the inner divertor. While the overall power flow to the divertor is similar to the case when drifts and current are neglected, the structure and dynamics of the plasma is considerably different.

Acknowledgments

This work was performed under the auspices of the U.S. Department of Energy by the University of California Lawrence Livermore National Laboratory under contract No. W-7405-Eng-48.

References

[1] ITER Physics Basis, in Nucl. Fusion **39** (1999), Chapt. 4, 2391.

[2] R. Schneider, et al., in Fusion Energy 1996 (Proc. 16th Int. Conf., Montreal, 1996), Vol. 2, IAEA, Vienna (1997) 465.

[3] T.D. Rognlien, J.A. Crotinger *et al.*, J. Nucl. Mat., **241-243** (1997) 590.

[4] A.V. Chankin, J. Nucl. Mater. **241-243** (1997) 199.

[5] T.D. Rognlien, D.D. Ryutov, N. Mattor, and G.D. Porter, Phys. Plasmas **6** (1999) 1851.

[6] M.J. Schaffer **et al.**, Phys. Plasmas **8** (2001) 2118.

[7] S.I. Braginskii, Transport processes in a plasma, *Reviews of Plasma Physics*, Vol. 1, Ed. M.A. Leontovich (Consultants Bureau, New York, 1965), p. 205.

[8] R.H. Cohen and D.D. Ryutov, Comm. Plasma Phys. Contr. Fusion **16** 255 (1995); Phys. Plasmas **2** 2011 (1995).

[9] R.H. Cohen and T.D. Rognlien, Contrib. Plasma Phys. **34** (1994) 198.

[10] O. Batishchev *et al.*, Phys. Plasmas **4** (1997) 1672.

[11] V.P. Pastukhov, Nucl. Fusion **14** 3 (1973).

[12] T.D. Rognlien and T.A. Cutler, Nucl. Fusion **20** (1980) 1003.

Figure captions

(1) The poloidal electron temperature profiles for a poloidal flux surface 2 mm outside the separatrix at the midplane at three times following an increase of the anomalous diffusion coefficients by a factor of 20.
(2) Plasma density profiles on the outer plate for two times in the ELM simulation for cases without and with cross-field drifts and current.
(3) Total poloidal heat flux to the inner and outer divertor plates for $t =$ 200 μs into the ELM.

(4) Vectors of ion plasma particle flux×area near the outer separtrix for (a), $t = 0$ μs and (b), $t = 27$ μs with cross-field drifts and current on. The solid line is the magnetic separatrix.
(5) Calculated $e\phi_s/T_e$ profiles at the inner and outer divertor plates at two times with cross-field drifts and current on.

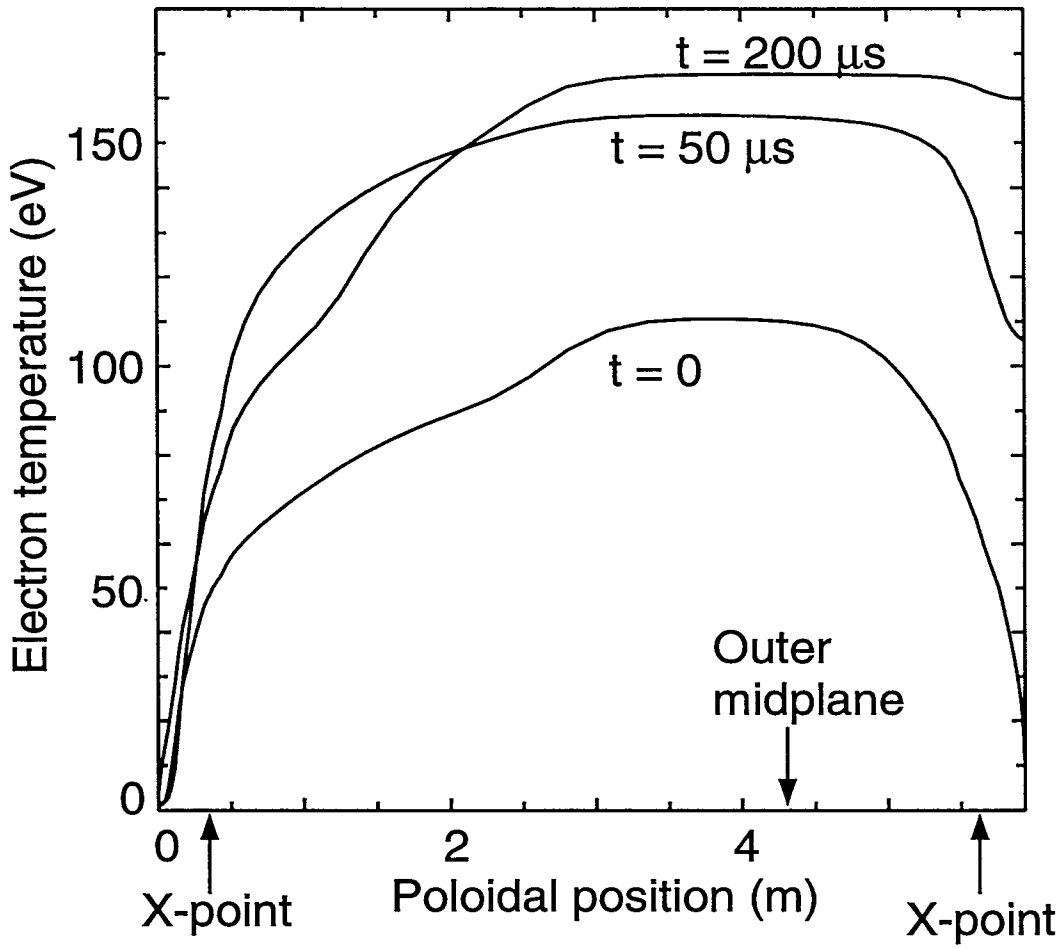
t = 200 μs
t = 50 μs
t = 0
150
100
50
0
Electron temperature (eV)
Outer
midplane
0
2
4
X-point
Poloidal position (m)
X-point

Fig. 1

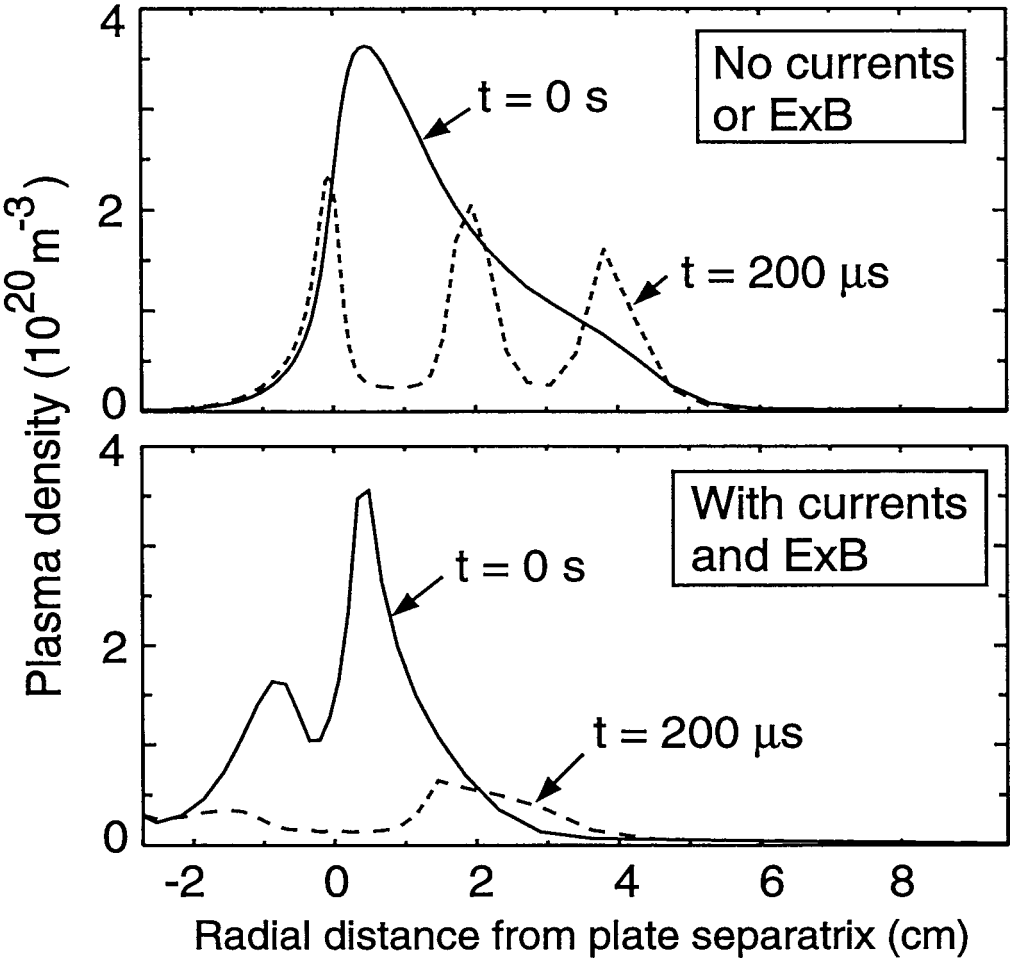
No currents
or ExB
t = 0 s
t = 200 μs
With currents
and ExB
t = 0 s
t = 200 μs
Plasma density (10^{20} m^{-3})
Radial distance from plate separatrix (cm)
0
2
4
-2
0
2
4
6
8

Fig. 2

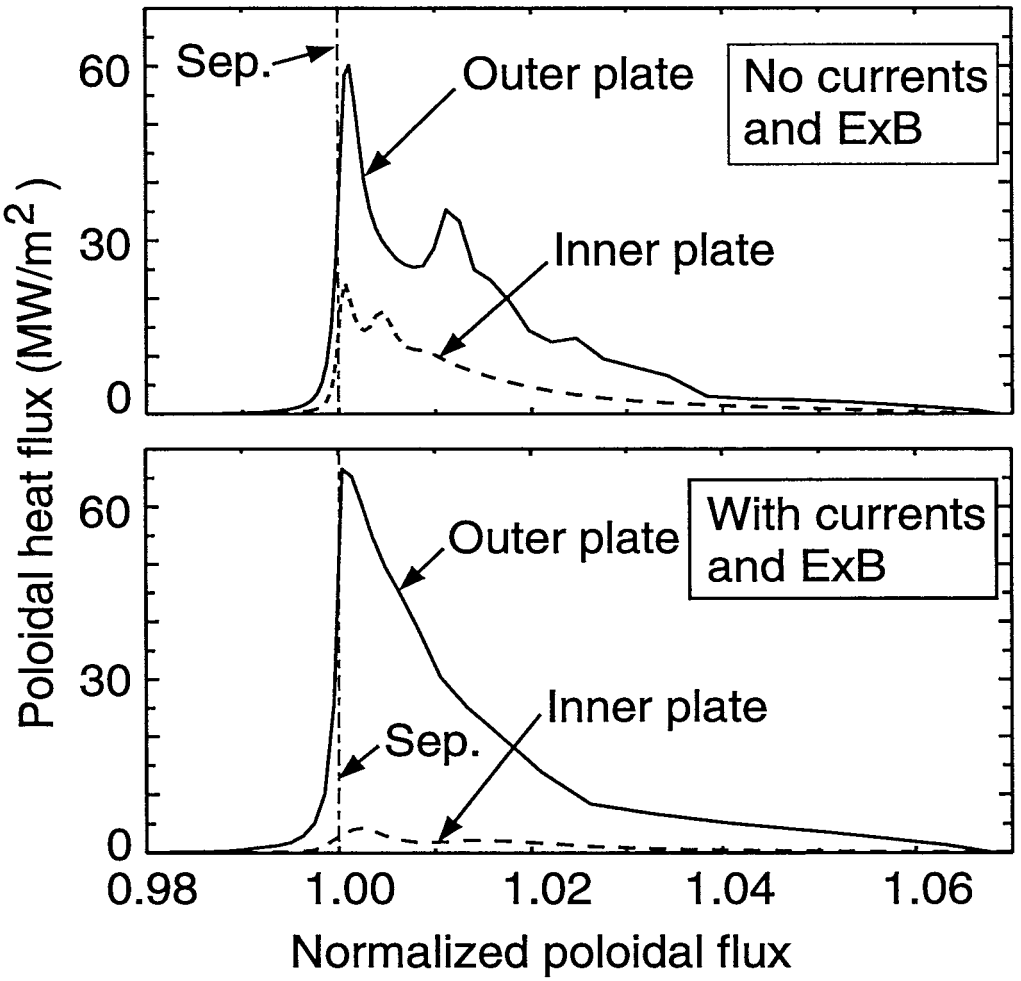
Sep.
Outer plate
No currents
and ExB
Inner plate
60
30
0
Outer plate
With currents
and ExB
Inner plate
Sep.
60
30
0
0.98
1.00
1.02
1.04
1.06
Poloidal heat flux (MW/m^2)
Normalized poloidal flux

Fig. 3

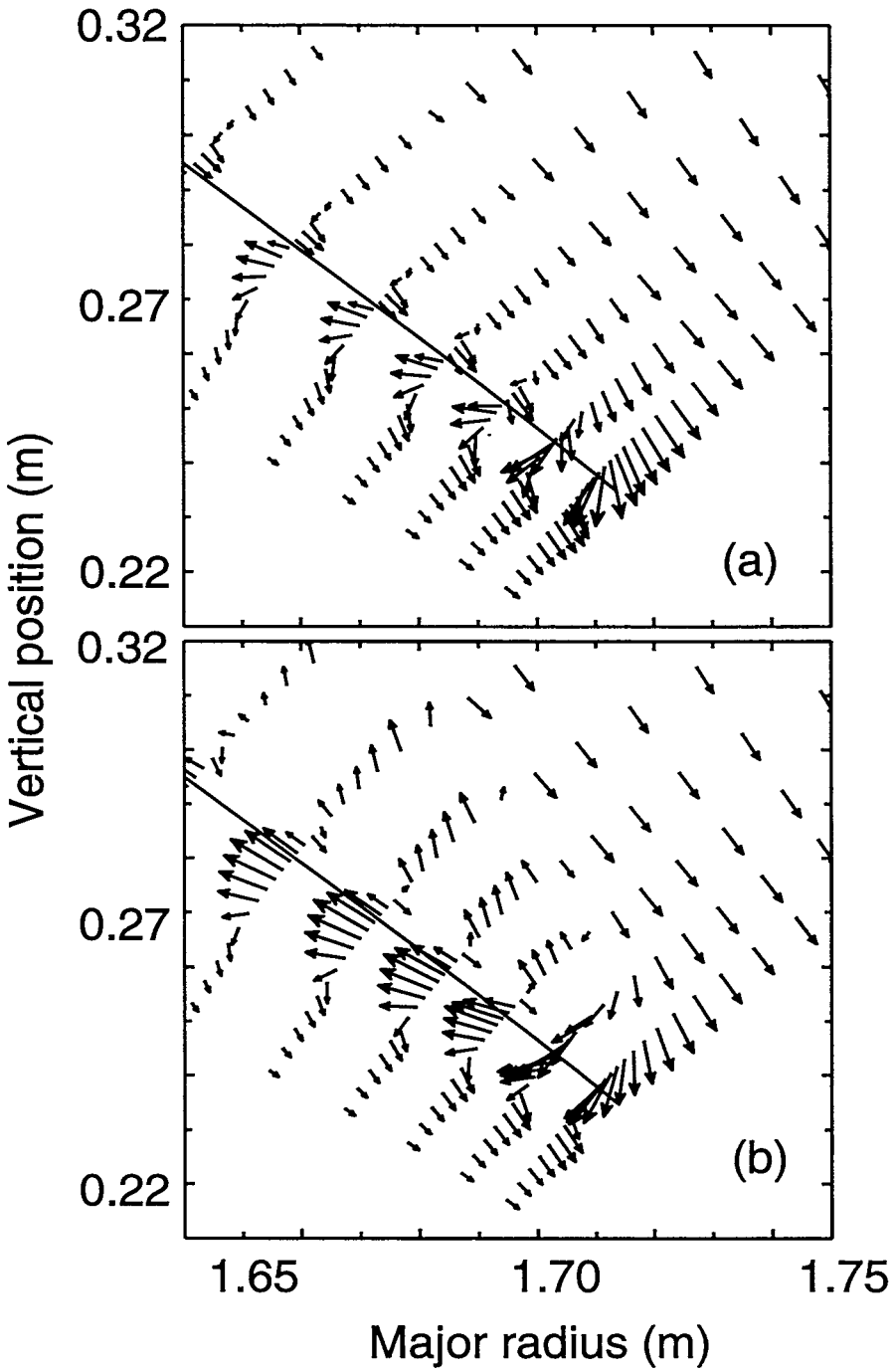
0.32
0.27
0.22
(a)
0.32
0.27
0.22
(b)
Vertical position (m)
1.65
1.70
1.75
Major radius (m)

Fig. 4

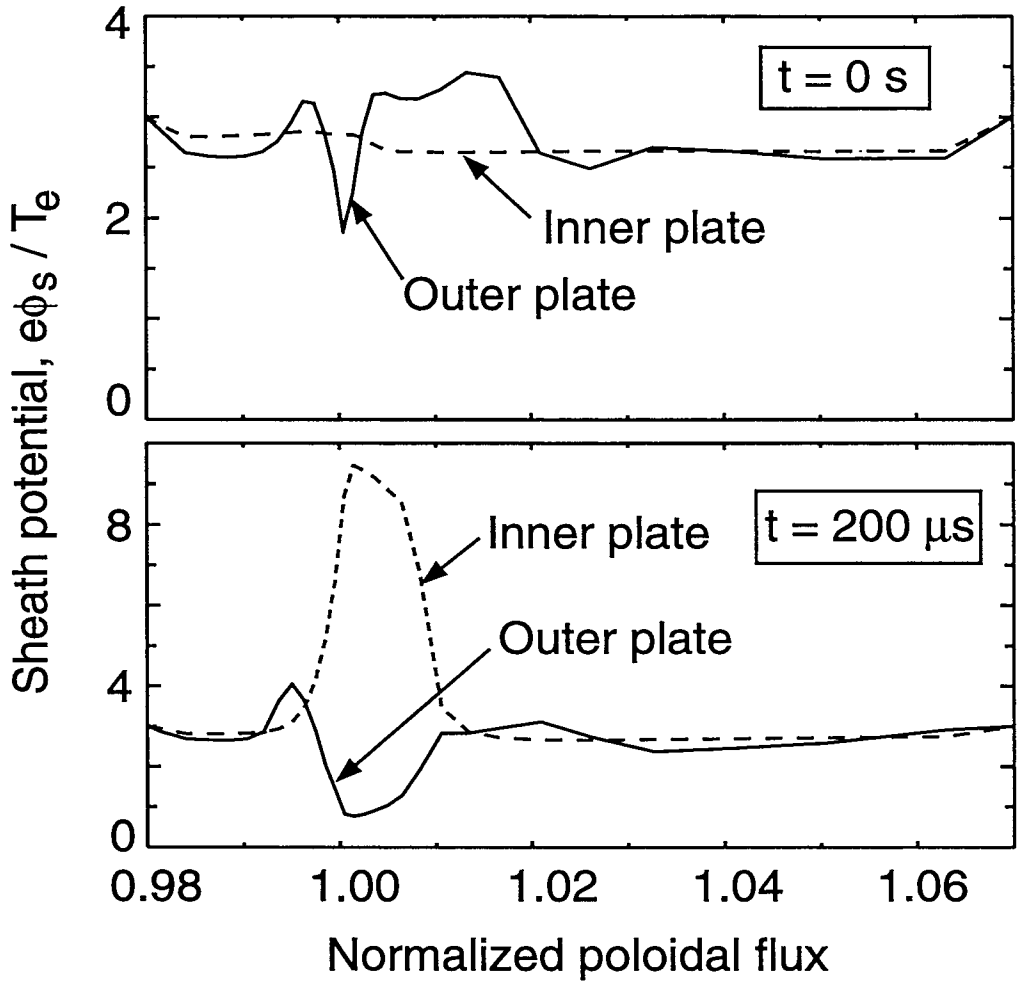
4
2
0
t = 0 s
Inner plate
Outer plate
8
4
0
Inner plate
t = 200 μs
Outer plate
0.98
1.00
1.02
1.04
1.06
Normalized poloidal flux
Sheath potential, eφs / Te

Fig. 5